Global Change Biology

Global Change Biology (2012), doi: 10.1111/j.1365-2486.2011.02629.x

Seasonal carbon dynamics and water fluxes in an Amazon rainforest

YEONJOO KIM*†, RYAN G. KNOX‡, MARCOS LONGO§, DAVID MEDVIGY¶, LUCY R. HUTYRA‖, ELIZABETH H. PYLE§, STEVEN C. WOFSY§, RAFAEL L. BRAS** and PAUL R. MOORCROFT*

*Department of Organismic and Evolutionary Biology, Harvard University, Cambridge, MA 02138, USA, †Korea Adaptation Center for Climate Change, Korea Environment Institute, Seoul 122-706, Korea, ‡Department of Civil and Environmental Engineering, Massachusetts Institute of Technology, Cambridge, MA 02139, USA, §Department of Earth and Planetary Sciences, Harvard University, Cambridge, MA 02138, USA, ¶Department of Geosciences, Princeton University, Princeton, NJ 08544, USA, ‖Department of Geography and Environment, Boston University, Boston, MA 02215, USA, **Departments of Civil and Environmental Engineering and of Earth and Atmospheric Sciences, Georgia Institute of Technology, Atlanta, GA 30332, USA*

Abstract

Satellite-based observations indicate that seasonal patterns in canopy greenness and productivity in the Amazon are negatively correlated with precipitation, with increased greenness occurring during the dry months. Flux tower measurements indicate that the canopy greening that occurs during the dry season is associated with increases in net ecosystem productivity (NEP) and evapotranspiration (ET). Land surface and terrestrial biosphere model simulations for the region have predicted the opposite of these observed patterns, with significant declines in greenness, NEP, and ET during the dry season. In this study, we address this issue mainly by developing an empirically constrained, light-controlled phenology submodel within the Ecosystem Demography model version 2 (ED2). The constrained ED2 model with a suite of field observations shows markedly improved predictions of seasonal ecosystem dynamics, more accurately capturing the observed patterns of seasonality in water, carbon, and litter fluxes seen at the Tapajos National Forest, Brazil (2.86°S, 54.96°W). Long-term simulations indicate that this light-controlled phenology increases the resilience of Amazon forest NEP to interannual variability in climate forcing.

Keywords: Amazon, ecosystem model, evapotranspiration, light-controlled phenology, net ecosystem productivity, root water uptake, tropical forests

Received 18 September 2011 and accepted 19 October 2011

Introduction

The Amazon rainforest accounts for 50% of undisturbed tropical rainforest, and plays a critical role in the Earth's water and carbon cycles. Recent terrestrial biosphere modeling studies indicate that anthropogenic climate change is likely to give rise to profound changes in the structure, composition, and functioning of tropical forests over the coming century, and that significant biophysical and biogeochemical biosphere-atmosphere feedbacks are likely to occur as a result of these changes (Cox *et al*., 2000; Huntingford *et al*., 2008). In particular, in the case of Amazon forests, the studies suggest that both climate and deforestation-induced changes in tropical forests will feedback onto regional and global climate, causing reductions in regional precipitation, increases in regional surface temperature, and increases in the rate at which CO_2 builds-up in the atmosphere.

Correspondence: Paul R. Moorcroft, tel. + 1 617 496 6744, fax: + 1 617 495 5667, e-mail: paul_moorcroft@harvard.edu

However, recent observational studies call into question the accuracy of current terrestrial biosphere model predictions for the Amazon (Saleska *et al*., 2003). Satellite measurements indicate that canopy greenness in the Amazon is negatively correlated with precipitation patterns with increased greenness and higher productivity occurring during the dry season (Huete *et al*., 2006, 2008; Myneni *et al*., 2007). In addition, flux tower measurements indicate that the canopy greening that occurs during the dry season is associated with increased net ecosystem productivity (NEP) and evapotranspiration (ET) during the dry season (Hutyra *et al*., 2007). This pattern of observed variability is in direct opposition to prior process-based land surface and ecosystem model predictions, in which ET and NEP both decline during the dry season, in phase with precipitation (Saleska *et al*., 2003; Werth & Avissar, 2004).

Subsequently, some terrestrial biosphere and land surface models have sought to address this discrepancy by incorporating parameterizations for the root water uptake into their model formulations. Specifically, Lee

© 2011 Blackwell Publishing Ltd

et al. (2005) incorporated the hydraulic redistribution into the Community Land Model (CLM), and showed that the inclusion of hydraulic redistribution into CLM enabled it to capture the observed seasonality of ET (i.e., maximum ET in the dry season) in the Amazon basin; however, photosynthesis still declined during the dry season. Subsequently, Baker *et al.* (2008) modified the Simple Biosphere model to include a deeper soil column, a dynamic root water uptake function, a root hydraulic redistribution parameterization, and sunlit and sunshade canopy fractions into the radiative transfer parameterization. They found that collectively these changes in model parameterizations yielded a seasonal pattern of NEP similar to the observed NEP seasonality.

The seasonal dynamics of leaf emergence and leaf fall (i.e., leaf phenology) have also been suggested as a possible mechanism to explain the dry-season maxima of carbon and water fluxes (Xiao *et al.*, 2005; Hutyra *et al.*, 2007). Field observations in the Amazon forests showed that litterfall peaked early in the dry season when radiation is maximized (Luizao, 1989; Rice *et al.*, 2004). Water availability has been proposed as the proximal environmental trigger for the increases in leaf litter fluxes during the dry season in Amazon rainforests; however, several experimental studies, including a study in the tropical moist forest on Barro Colorado Island, Panama (Wright & Cornejo, 1990), and a study in the gallery and montane forests of Chapada Diamantina, Brazil (Miranda *et al.*, 2011), showed no relationship between water stress and leaf litter fall. Following the peak in litter fall, new leaves, which have higher photosynthetic efficiency (Freeland, 1952), flush in the dry season when radiation levels are higher (Van Schaik *et al.*, 1993; Wright & Van Schaik, 1994; Rivera *et al.*, 2002; Xiao *et al.*, 2005; Huete *et al.*, 2006). The higher photosynthetic capacity of young leaves may thus account for the increased rate of carbon assimilation observed during the dry season.

The focus of this study is on accounting for the observed seasonal pattern leaf green-up and resulting carbon fluxes in the dry season, rather than on the response of Amazonia forest to episodic drought (Saleska *et al.*, 2007; Samanta *et al.*, 2010). These responses may be related, however, particularly if the seasonal and interannual responses are induced by similar environmental triggers.

As mentioned before, observed seasonality of carbon and water fluxes may be attributed to one or both of the root water dynamics (including hydraulic redistribution, dynamic root functioning or deep root system) and the leaf phenology. For example, Xiao *et al.* (2005) hypothesized that seasonally moist tropical forests have evolved two adaptive mechanisms for strong seasonal variations of light and water: (1) deep root systems for access to water in deep soils, and (2) leaf phenology for access to light. They showed that the satellite-derived Enhanced Vegetation Index (EVI) captured the seasonal dynamics of leaf phenology (i.e., its increase in the dry season) and land surface water index (LSWI) indicated no water stress in the dry season during their study period. Furthermore, they could simulate the observed seasonality of carbon flux (i.e., its dry-season peak) based on satellite-derived EVI and LSWI in addition to site-specific climate data of air temperature and photosynthetically active radiation. As such, the light-controlled phenology as well as the root water dynamics can play a crucial role in observed seasonal variations of fluxes in Amazon rainforest, but most modeling studies have focused on the root water dynamics (Lee *et al.*, 2005; Zheng & Wang, 2007; Baker *et al.*, 2008).

In this analysis, we evaluate the patterns of seasonality in carbon and water fluxes predicted by the original parameterization of the Ecosystem Demography model version 2 (ED2) biosphere model against eddy-flux measurements and forest inventory measurements obtained at Tapajos National Forest (TNF). After evaluating the predictions of the original model parameterization, we use a subset of the measurements to develop and constrain a new light-controlled phenology submodel, and show that the constrained ED2 is able to correctly capture the observed seasonal variation in carbon and water fluxes as well as litter fluxes.

Methods

ED2 terrestrial biosphere model

ED2 is an integrated terrestrial biosphere model incorporating hydrology, land surface biophysics, vegetation dynamics and soil carbon and nitrogen biogeochemistry (Medvigy *et al.*, 2009). The fast timescale fluxes of carbon, water, and energy between the land surface and the atmosphere are captured using leaf photosynthesis and soil decomposition modules coupled to a multileaf layer and multisoil layer biophysical scheme. As seen in Fig. 1, each grid cell is divided into a series of tiles, each containing a size-stratified, functionally diverse, plant canopy (Fig. 1a). For each tile, ED2 computes the multilayer canopy fluxes of water, internal energy, and carbon (Fig. 1b). Like its predecessor, ED2 tracks long-term changes in the biophysical, ecological, and biogeochemical structure of the land surface using a system of size- and age-structured partial differential equations that capture the dynamic changes in the subgrid scale structure and composition of the ecosystems within each grid cell, which result from the fast-time scale ecosystem dynamics playing out over yearly, decadal, and century timescales (Moorcroft *et al.*, 2001; Moorcroft, 2003, 2006). This system of equations is able to make realistic projections of both short-term canopy fluxes and long-term vegetation dynamics, and can incorporate the impacts of

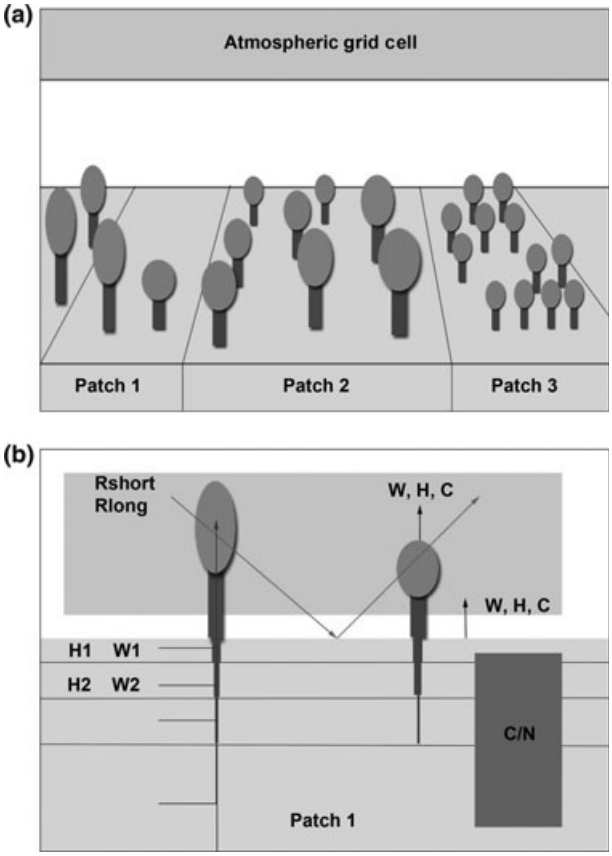

Fig. 1 Ecosystem Demography model version 2 (ED2) model structure and processes: (a) each grid cell is divided into a series of subgrid tiles that capture subgrid scale heterogeneity in canopy structure. (b) ED2 computes the multilayer canopy fluxes of water (W), internal energy (H), and carbon (C) within each subgrid scale tile.

subgrid scale disturbances on the structure and function of the land surface within each grid cell (Medvigy *et al.*, 2009). This includes natural disturbances, such as wind-throw and natural fires, and anthropogenic disturbances, such as land-conversion and anthropogenic fire activity (e.g., see Hurtt *et al.*, 2002; Albani *et al.* 2006).

The initial parameterization of Amazonian plant functional diversity used in this analysis was taken from Moorcroft *et al.* (2001), which represented the dynamics of C_4 grasses plus early-successional, mid-successional, and late-successional tropical tree types that differ in their photosynthetic and biophysical properties. As described in Moorcroft *et al.* (2001), the three types of tropical trees are designed to approximate a continuum of successional life-history strategies found within tropical forest canopies, ranging from fast-growing pioneer trees that have high mortality rates to slower-growing longer lived, late-successional tropical tree species.

Tapajos site measurements

The flux tower and forest inventory measurements used in this study came from the TNF (2.86°S, 54.96°W; Para, Brazil) near 67 km of the Santarem-Cuiaba highway (Hutyra *et al.*, 2007). Flux tower measurements using the eddy covariance technique were commenced in April 2001 and decommissioned in January 2006 (Hutyra *et al.*, 2007). Biometric plots (four 50 × 1000 m transects adjacent to the tower) were established in July 1999 and have been surveyed in 1999, 2001, and 2005 (Rice *et al.*, 2004; Pyle *et al.*, 2008). Trees $\geq$35 cm diameter at breast height (dbh) of 949 individuals were identified along four transects, and trees $\geq$10 cm dbh were identified along the narrower transects (four 10 × 1000 m) in the middle of larger transects (see figure 1 in Rice *et al.*, 2004). This site lies at the dry end of the climate zone supporting evergreen forests in the Amazon, and is classified as a primary forest with few anthropogenic disturbances other than small-scale hunting. The mean annual precipitation at the TNF is 1920 mm with a mean dry season length (months with <100 mm precipitation) is about 5 months, typically from July 15 to December 15.

Analysis

We performed an initial 4-year simulation (hereafter referred to as 'ORIG') for the period 2002 through 2005, using the parameterization directly from that of the original ED ecosystem model for Amazonia (Moorcroft *et al.*, 2001), reflecting our prior quantitative understanding of vegetation dynamics within the region. The model was forced with hourly measurements of short- and longwave radiation, air temperature, precipitation, relative humidity, wind speed, and air pressure, which have been recorded at the Tapajos flux tower since April 2001, except for short- and longwave radiation, which was specified from a separate dataset collected at a nearby location (D. Fitzjarrald, personal communication). Occasional gaps in the climatological data caused by power failures, recalibration periods, and extreme precipitation events were filled with median-filtered data following the procedure of *Stöckli et al.* (2008).

The soil column was configured with a 6 m soil depth with 14 layers and a free-drainage lower boundary to realistically represent the water available for canopy transpiration since observations indicate that in the Tapajos forest tree roots can be found to depths in excess of 10 m (Nepstad *et al.*, 1994; Bruno *et al.*, 2006). Details about soil depth and root soil water uptake function in ED2 will be discussed in 'Plant root water uptake' section. Soil texture was prescribed based on the field data from Silver *et al.* (2000). Initial soil moisture was set near saturation because the model simulations started in July (i.e., during the wet season) due to the data availability of ecosystem composition data, and soil temperature was equated to atmospheric air temperature. An 8-year model equilibration was then performed to minimize any transient dynamics arising from the soil moisture and temperature initial conditions.

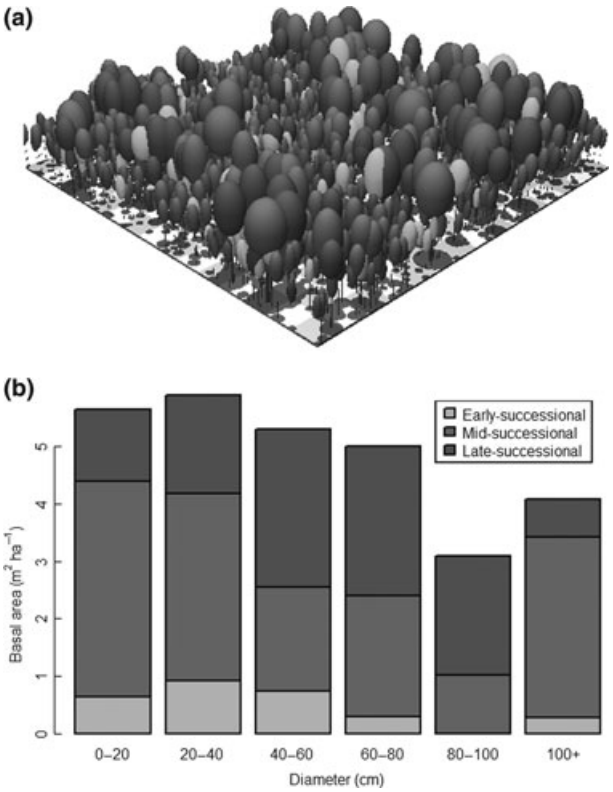

Fig. 2 (a) Ecosystem composition in the Tapajos National Forest flux tower footprint: early-successional (light green), mid-successional (green), and late-successional trees (dark green). (b) Distribution of basal area of the three different plant functional types across tree diameter classes.

Ecosystem composition was initialized from the forest inventory transects conducted in the footprint of the Tajajos 67 km eddy-flux tower for all trees larger than 10 cm dbh in July 2001 (see 'Tapajos site measurements'). The different tree species were grouped to into the early-, mid-, and late-successional types based on their woody density (Chave *et al.*, 2006). The forest composition and structure determined from the 2001 census is illustrated in Fig. 2. As can be seen in the figure, early- mid- and late-successional trees, respectively, comprise 12%, 57%, and 31% of the forest basal area. Because the canopy-gap scale distribution of times since last disturbance within the tower footprint is not known, horizontal heterogeneity in canopy composition was represented explicitly, by grouping the inventoried plots into series of 40 distinct subgrid scale tiles based on their similarity in vertical canopy structure and composition. The compositional profile within each tile was represented explicitly, using the diameter of each tree (diameter at breast height, DBH) as a measure of its size and using species wood density values to assign each tree to its corresponding plant functional type (PFT). The ecophysiological and life-history differences between the PFT are listed in Table 1. Combining the forest inventory measurements with the ED2 allometric functions and specific leaf area values yields an implied canopy LAI of 3.7. This value is lower than ground observations of 4.5–5.6 found at a neighboring field study site at Santarem (Domingues *et al.*, 2005). This difference likely arises from the allometric relationships between DBH and leaf biomass that are based on allometric data collected in Columbian and Venezuelan tropical forests (Saldarriaga *et al.*, 1988) (the canopy LAI is simply the sum of this number over all trees within the canopy, which, as noted before, is prescribed from observations). Since the error on LAI measurements is generally agreed to be ca. 20% the model is, however, within the lower error bound (an LAI of 3.6), the existing allometric functions were retained in this study.

Results from this initial ED2 model simulation (shown in Figs 5–8) indicate the following errors in the model predictions of carbon fluxes, water fluxes, and tree growth and mortality:

1 Opposite seasonality of monthly NEP, daytime NEP and nighttime NEP, for which the correlation coefficients with the observed fluxes are −0.76, −0.58, and −0.73, respectively.
2 Slightly overestimated ET with the RMS error of 11 mm month^{-1}, ~12% of observed flux.
3 Significantly underestimated magnitude and seasonality of the litter flux. The predicted mean litter flux

Table 1 Ecophysiological and life-history parameters for the plant functional types represented in the ED2 model simulations

		Tropical tree		
Property	C4 grass	Early-successional	Mid-successional	Late-successional
V_{m0} (μmol m^{-2} s^{-1})*	12.5	18.75	12.5	6.25
Leaf lifespan (year)	2	1	0.5	0.33
Wood density (g cm^{-3})	0.4	0.4	0.6	0.87
Specific leaf area (m^2 kgC^{-1})	27	22	17	15
Density independent mortality (yr^{-1})	0.037	0.037	0.029	0.0

*V_{m0} values in the initial model are provided here; in the optimized model, V_{m0} is a function of leaf lifespan (see Eqn 2). ED2, Ecosystem Demography model version 2.

is ~30% of the observed, and the predicted seasonal variation is ~1% of the observed seasonal variation in litter flux.

4 Overestimated growth and mortality, with RMS errors of 0.15 m^2 ha^{-1} yr^{-1} (~26% of the observed) and 0.05 m^2 ha^{-1} yr^{-1} (~9% of the observed), respectively.

Model reformulation: light-controlled leaf dynamics

The original phenology model taken from Moorcroft *et al.* (2001) is a simple drought-deciduous phenology scheme similar to those used in other biosphere models (e.g., Foley *et al.*, 1996), in which plants drop their leaves only if plant water availability, as measured by relative soil moisture (θ), falls below a critical value ($\theta < 0.2$); otherwise, leaf biomass turns over at a constant background rate.

Motivated by the observations that leaf litterfall increases significantly as radiation increases during the dry season (Fig. 3), we developed a light-controlled phenology scheme, in which the rate of leaf turnover of each PFT (α_{leaf}) is assumed to increase linearly with increasing levels of incoming radiation (Fig. 4a), that is,

$$\alpha_{\text{leaf}}^{(i)}(z,a) = (\alpha_1 \bar{I}(z,a) + \alpha_2) \cdot \alpha_0^{(i)}, \qquad (1)$$

where $\bar{I}$ (z, a) is the average incoming radiation level over the past 10-day period, experienced by the plant of type i, size z in tile a, and $\alpha_0{}^{(i)}$ is the intrinsic leaf lifespan of PFT i. Leaf trait correlation studies (Wright *et al.*, 2004) indicate that leaf photosynthetic capacity (V_m) decreases with increasing leaf longevity (LL), the inverse of the leaf turnover rate (α_{leaf}). The observational dataset of *Wright et al.* (2004) was therefore used to specify a sigmoidal relationship between V_m and LL:

$$V_m^{(i)}(z,a) = \frac{V_m^{\text{amp}}}{\left(1 + \left(\frac{\text{LL}^{(i)}(z,a)}{\text{LL}^{\text{trans}}}\right)^{V_m^{\text{slope}}}\right)} + V_m^{\min}, \qquad (2)$$

where $V_m^{\min}$ and $V_m^{\min} + V_m^{\text{amp}}$, respectively, control the minimum and maximum leaf photosynthetic capacity; LL^{trans} determines the leaf lifespan at which leaf photosynthetic capacity declines to $V_m^{\min} + V_m^{\text{amp}}/2$; and V_m^{slope} controls the rate at which leaf photosynthetic capacity declines with increasing leaf lifespan (Fig. 4b). Note that the Wright *et al.* (2004) relationship described variation in photosynthetic capacity between species. Here, we use the above relationship both to define differences in leaf photosynthetic capacity between the early-, mid- and late-successional PFT within the model and to describe how seasonal variation in leaf lifespan results in associated changes in photosynthetic capacity. Our rationale for this is that, as described in the Introduction, empirical observations imply a similar qualitative relationship between seasonal leaf turnover rates and leaf photosynthetic capacity. The use of the same quantitative relationship is, however, solely based on parsimony.

Assuming the leaf biomass pool remains in approximate dynamic equilibrium (that is, Eqn 1 applies throughout the year) then as incoming solar radiation increases leaf longevity will decline and photosynthetic capacity will increase.

Together Eqns (1) and (2) give rise to seasonal variation in leaf longevity and photosynthetic capacity,

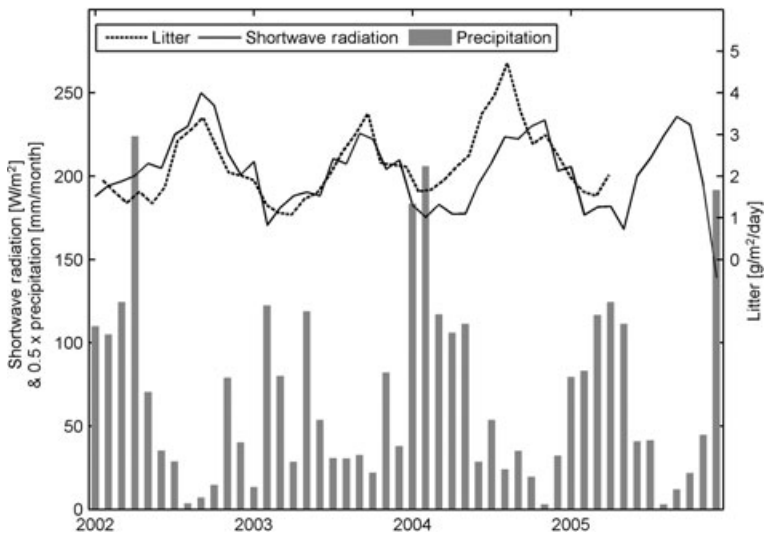

Fig. 3 Observed patterns of radiation (solid line), litter fluxes (dash line), and precipitation (gray bars) in the Tapajos National Forest flux tower site (data from *Hutyra et al.*, 2007).

© 2011 Blackwell Publishing Ltd, *Global Change Biology*, doi: 10.1111/j.1365-2486.2011.02629.x

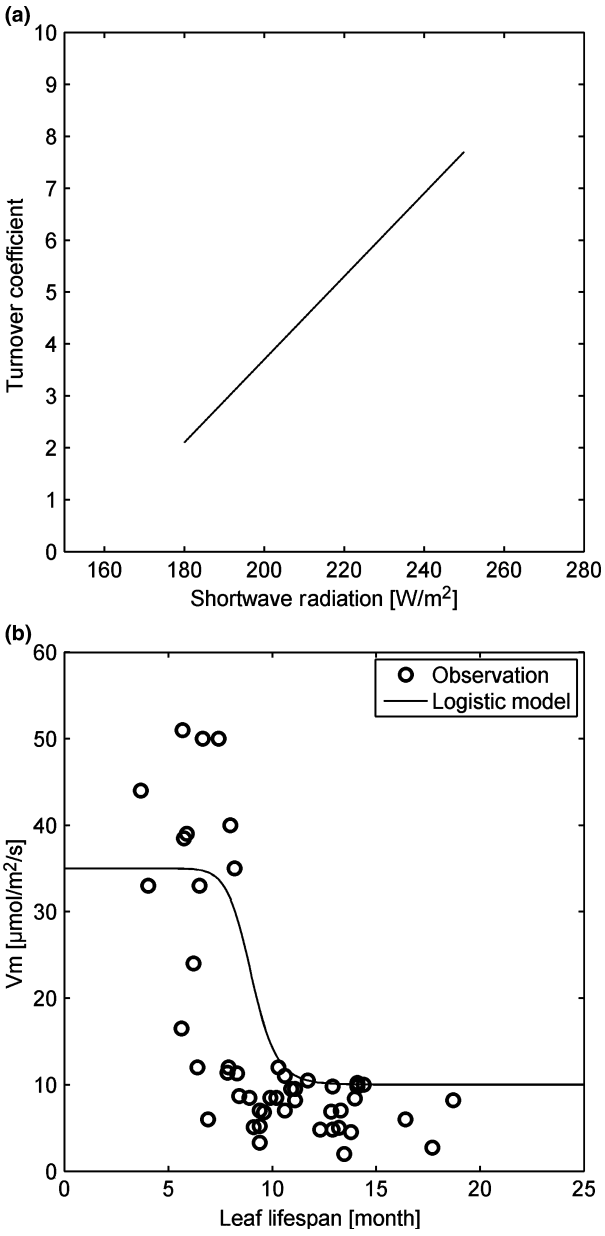

Fig. 4 Schematic diagram for the mechanistic light-controlled phenology model: (a) the rate of leaf turnover (α_{leaf}) increases linearly in relation to incoming levels of radiation (Eqn 1). (b) The relationship between the photosynthetic capacity (V_m) and leaf lifespan (LL) is represented with a logistic model fit (black line) to the *Wright et al.* (2004) measurements of photosynthetic performance (black open circles).

with concomitant increases in leaf turnover rate and leaf photosynthetic rates during the dry season when incoming radiation levels are higher. The new phenology model has two additional parameters, α_1 and α_2 in Eqn (1), which were constrained as part of the model optimization explained in 'Model optimization' section.

Model optimization

We used ecosystem measurements from a 2-year period, July 2002–June 2004, which included a relatively dry year and a relatively wet year, to constrain eight model parameters. The dry year (July 2002–June 2003) had mean precipitation rates of 53 and 130 mm month^{-1} for the dry (July to November) and wet seasons (December to June), respectively. The wet year (July 2003–June 2004) had mean precipitation rates of 79 mm month^{-1} and 225 mm month^{-1} for the dry and wet seasons, respectively (see Fig. 3). The eight model parameters, their associated uncertainties, and the covariances between parameters, were estimated by fitting the model's predictions for the July 2002–June 2004 period to the observational datasets listed in Table 2, using the method of maximum likelihood (Edwards, 1972). Following Mahadevan *et al.* (2008) and Medvigy *et al.* (2009), the effects of photosynthesis vs. effects of plant and heterotrophic respiration were distinguished by separating NEP into day- and night-time components, thereby improving the ability to correctly constrain the model's predictions of both the respiratory and photosynthetic components of the ecosystem's net carbon fluxes.

The eight parameters that were constrained with the observational data included the new two parameters of the light-controlled phenology model (Eqn 1 in 'Model reformulation: light-controlled leaf dynamics' section) to correct the underestimated magnitude and seasonality of litter and the incorrect pattern of seasonality in daytime NEP. The water and temperature dependency parameters of the soil decomposition model were also included (W_{opt} and w_1 in Eqn A1 and Q_{10} in Eqn A2), since these significantly impact the seasonality of ecosystem respiration and thus NEP. Since changes in plant photosynthesis and respiration, in turn, influence the plant's carbon balance and its resulting rates of diameter growth and mortality, we also included several important, relatively unconstrained, parameters influencing these processes, specifically, the allocation to fine roots relative to leaves (q in Eqn B1), the fine-root turnover rate (α_{root} in Eqn C2), and the intercept in the mortality function (m_1 in Eqn D1). Further details on the model fitting procedures can be found in Appendix E.

Results

Parameter estimates and uncertainty

The optimization significantly improved the model's goodness-of-fit to the observations. The log-likelihood (Eqn E1) increased from −16.0 in ORIG to −4.4 in the

Table 2 Summary of the observational datasets used to evaluate and constrain the ED2 model formulation

Source	Metric	Aggregation	Number of observations
Flux tower	Net ecosystem productivity (NEP)	Annual	2
		Monthly, daytime	24
		Monthly, nighttime	24
		Hourly, daytime	5825
		Hourly, nighttime	4625
	Litter	Annual	2
		Monthly	24
Forest inventory	Growth	PFT (early-; mid-; late-successional)	One for each
		DBH (10~35 cm; >35 cm)	aggregation
	Mortality	PFT (early-; mid-; late-successional)	One for each
		DBH (10~35 cm; >35 cm)	aggregation

DBH, diameter at breast height; ED2, Ecosystem Demography model version 2; PFT, plant functional types.

optimized model formulation (hereafter referred to as 'OPT'), and the associated change in the Akaike Information Criterion (AIC) (Eqn E2) from 44 to 25 indicated that this is a significantly improved goodness-of-fit despite the two additional parameters in the OPT model formulation.

The parameter estimates and the 95% (2σ) confidence bounds are given in Table 3. The parameters for the light-controlled phenology scheme were well constrained, with confidence bounds within 5% of maximum likelihood estimates. The optimization significantly changed the soil decomposition submodel (W_{opt} and w_1 in Eqn A1 and Q_{10} in Eqn A2). In particular, W_{opt}, the soil moisture level at which the decomposition rate is maximal (measured in terms of fraction of saturation), increased from 0.6 to 0.95 $m^3\ m^{-3}$, and w_1, the soil moisture dependency of decomposition, decreased from 5.0 to 2.2. The optimized W_{opt} value of 0.95 implies that the soil decomposition rate generally increases with increasing soil moisture until the saturation fraction becomes close to unity. The associated uncertainty of ± 0.22 on the value of W_{opt} implies lower bound of 0.73, a value which is only moderately higher than the value in ORIG. The high value of Wopt obtained in the model fitting is however consistent with the results of Medvigy *et al.* (2009), who found a similar increase in an model optimization exercise at a temperate forest site.

There were also changes in patterns of growth and mortality. Carbon allocation to fine-root relative to leaves (q in Eqn B1) decreased from 1.0 to 0.89, and the rate of fine-root turnover (α_{root} in Eqn C2) increased from 0.3 to 6.6 yr^{-1} (i.e. the mean longevity of fine roots decreased from 3 to 0.2 years). Estimates of fine-root longevities obtained in five empirical studies in broadleaf tropical forests indicate an observed range of 0.4 to 3.2 years (Gill and Jackson 2000). Two factors are likely to account for this difference. First, in the model, the fine-root turnover parameter also incorporates the production of short-lived root exudates that are typically not included in empirical measurements of fine-root longevity. Second, root dynamics remain a poorly understood component of terrestrial ecosystems: literature estimates indicate tremendous variation in

Table 3 Summary of the optimized model parameters

Parameter	Symbol	Initial value	Optimized value	2σ uncertainty	Reference (Equation No.)
Turnover parameter 1 (yr^{-1})	α_1	−8	−12.3	0.43	(1)
Turnover parameter 2 (yr^{-1})	α_2	0.05	0.08	0.002	(1)
Optimal soil moisture ($m^3\ m^{-3}$;fraction of saturation)	W_{opt}	0.6	0.95	0.22	(A1)
Soil moisture convexity parameter	w_1	5.0	2.2	4.8	(A1)
Temperature Q_{10}	q_{10}	2.1	2.5	1.3	(A2)
Allocation to fine-root relative to leaves	q	1	0.89	0.26	(B1)
Root turnover rate (yr^{-1})	α_{root}	0.3	6.6	1.6	(C2)
Density-dependent mortality parameter	m_1	10	0.03	0.08	(D1)

© 2011 Blackwell Publishing Ltd, *Global Change Biology*, doi: 10.1111/j.1365-2486.2011.02629.x

fine-root longevities, ranging from days to years, depending on root diameter (Gaudinski *et al.*, 2000; Matamala *et al.*, 2003), and the methods of estimating tree root dynamics in the field are hampered by large spatial variability, making it difficult to accurately quantify root biomass and turnover rates in the field (Trumbore *et al.*, 2006). Interestingly, Medvigy *et al.* (2009) obtained a similar magnitude increase in the rate of fine-root turnover (from 0.3 to 5.1) in a model fitting exercise at a temperate forest site.

The density-dependent mortality parameter (m_1 in Eqn D1) that controls how a plant's mortality rate increases in response to low daily carbon balance (i.e., the net daily carbon uptake relative to what it would be in full sun), decreased significantly from 10 to 0.03. These results suggest that mortality rates decreased particularly for the trees in the understory.

Seasonal variation of fluxes and vegetation dynamics

Figure 5(a) compares the simulated vs. observed litter fluxes. Litter fluxes in ORIG do not have any noticeable seasonal variation because the canopy leaf biomass turns over at a constant, prescribed background rate. In OPT, the model captures more closely the observed seasonal variability of litter fluxes, responding to incoming solar radiation as a result of Eqn (1). The magnitude of the seasonality in litter fluxes is accurate during the months of the fitting period (July 2002–June 2004), but is underestimated in subsequent months. Nonetheless, the correlation between the predictions and the observations is considerably improved from +0.33 (ORIG) to +0.63 (OPT). The predicted mean litter flux also improved from 30% to 77% of the observed, and the predicted seasonality improved from 1% to 83% of the observed seasonal variation.

The seasonal variation in NEP (Fig. 5b) is also markedly improved the correlation coefficient increasing from −0.76 (ORIG) to +0.70 (OPT), and the RMS error decreasing from 0.95 tonC ha^{-1} month^{-1} (ORIG) to 0.29 tonC ha^{-1} month^{-1} (OPT). Examination of the partitioning between the diurnal and nocturnal NEP (Fig. 6a and b) shows that the optimized model captures the strong seasonal variation in photosynthetic assimilation as a result of the new phenology scheme (Eqns 1 and 2), and seasonality in respiration through the change in value of the optimal soil moisture parameter in the soil decomposition model. Similarly, the correlation coefficients between the model predictions and the observations also improve markedly, changing from −0.58 to +0.47 for the diurnal NEP and from −0.73 to +0.55 for the nocturnal NEP.

The ET fluxes in the ORIG simulation are reasonably similar to the observations, but are little changed in the

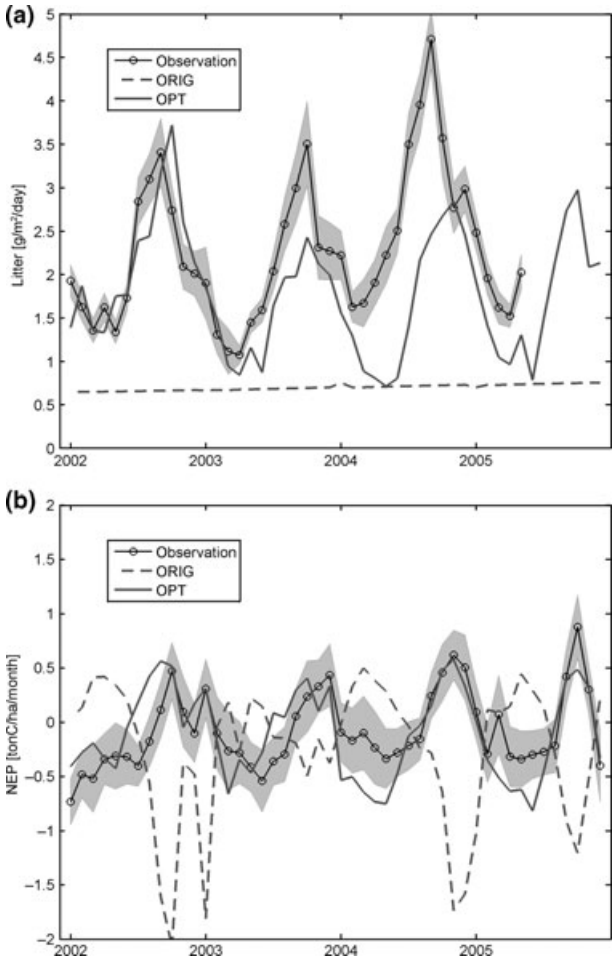

Fig. 5 Observed and predicted patterns of monthly (a) litter (g m^{-2} day^{-1}), and (b) net ecosystem productivity (NEP, tonC ha^{-1} month^{-1}). The black line shows the observations and the shaded area indicates the 2σ error. The dashed gray and solid gray lines, respectively, show the predictions of the ORIG and OPT model formulations.

OPT simulation (Fig. 7). In both ORIG and OPT, the model predictions are slightly higher than the observed ET, but the differences are relatively small, particularly given the known lack of energy closure in the eddy-flux measurements (Aranibar *et al.*, 2006; Baker *et al.*, 2008). Although their overall levels of ET were relatively similar, the partitioning of ET changed between the ORIG and OPT: the average magnitude of transpiration increased by 20% in OPT compared to ORIG, with the differences being greatest during the dry season when the new phenology parameterization results in higher carbon fluxes. While rate of transpiration is closely linked to the rate of canopy photosynthesis, the total ET is governed by the atmospheric forcing, specifically the atmospheric humidity and incoming radiation, and so the increase in transpiration associated with increase in

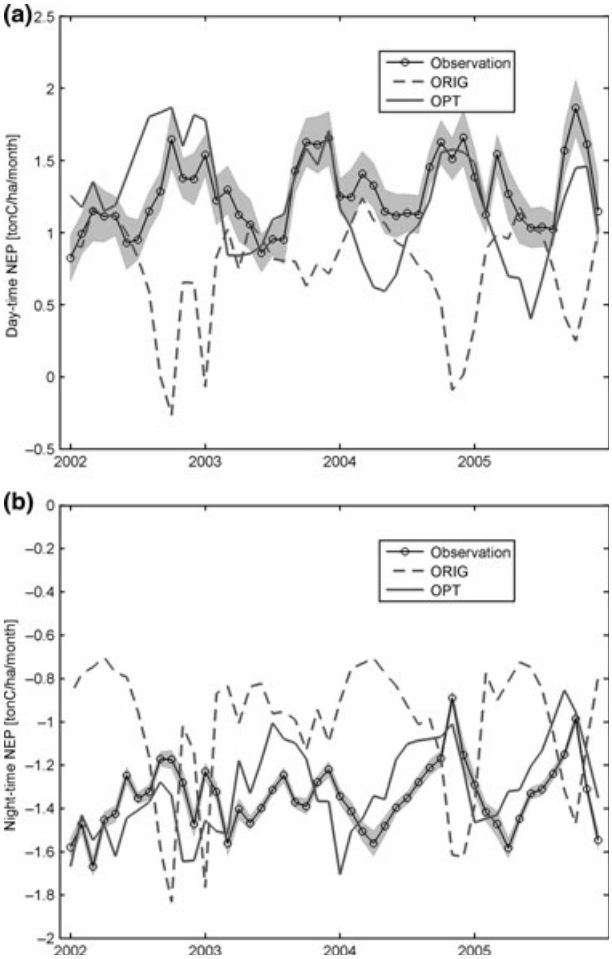

Fig. 6 Observed and predicted patterns of monthly (a) day-time net ecosystem productivity (NEP, tonC ha^{-1} $month^{-1}$) and (b) night-time NEP (tonC ha^{-1} $month^{-1}$). The black line shows the observations, and the shaded area indicates the 2σ error. The dashed gray and solid gray lines, respectively, show the predictions of the ORIG and OPT model formulations.

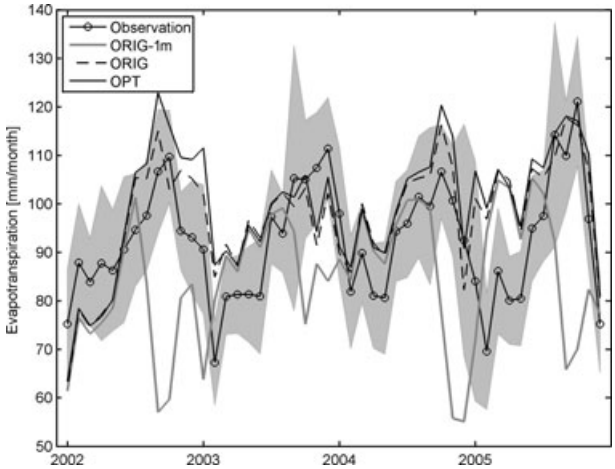

Fig. 7 Observed and predicted patterns of monthly evapotranspiration (mm $month^{-1}$). The black line shows the observations, and the shaded area indicates the 2σ error. The solid gray, dashed black, and solid black lines show the predictions of the ORIG-1 m, ORIG, and OPT model formulations.

photosynthesis, in OPT was accompanied by a corresponding decrease in the rate of evaporation (both ground and evaporation from the surface of leaves).

The observed rates of growth and mortality (Fig. 8) are constant throughout the simulation period since only two biometry measurements performed during this period, one in 2001 and the other in 2005, yielding a single, temporally averaged, growth and mortality. As noted earlier, the significant changes in gross primary productivity (GPP) resulting from the changes in leaf photosynthesis and turnover submodels have implications for rates of tree growth and mortality. Accordingly, the parameters related to slower-timescale growth and mortality dynamics (q in Eqn B1, α_{root} in Eqn C2, and m_1 in Eqn D1) were included in the parameter optimization. As shown in Table 3, α_{root} and m_1 changed significantly: α_{root} increased from 0.3 to 6.6, and m_1 decreased 10 to 0.03. Visual inspection of the model's predictions before and after optimization (Fig. 8) shows that the model's predictions of growth improved: the RMS error for growth decreased from 0.15 to 0.07 m^2 ha^{-1} yr^{-1}. However, the RMS error for mortality increased slightly, from 0.05 to 0.06 m^2 ha^{-1} yr^{-1}. Overall, the changes in growth and mortality were relatively modest, indicating that the changes in the growth and mortality parameters primarily reflected compensatory adjustments linked to the change in plant level GPP.

Discussion

Light-controlled phenology

In this study, a new light-controlled phenology scheme within ED2 was developed, parameterized, and tested against observations of canopy carbon, water and litter fluxes and accompanying growth and mortality dynamics at the TNF. As our results show, the optimized model with (1) the light-controlled phenology, (2) changes in other parameters (see 'Model optimization' section), and (3) the combination of deep soil configuration and dynamic root water uptake (see 'Plant root water uptake' section), is able to capture the observed pattern of seasonality in the patterns of carbon and water fluxes, in which both NEP and ET increase during the dry season (Hutyra *et al.*, 2007).

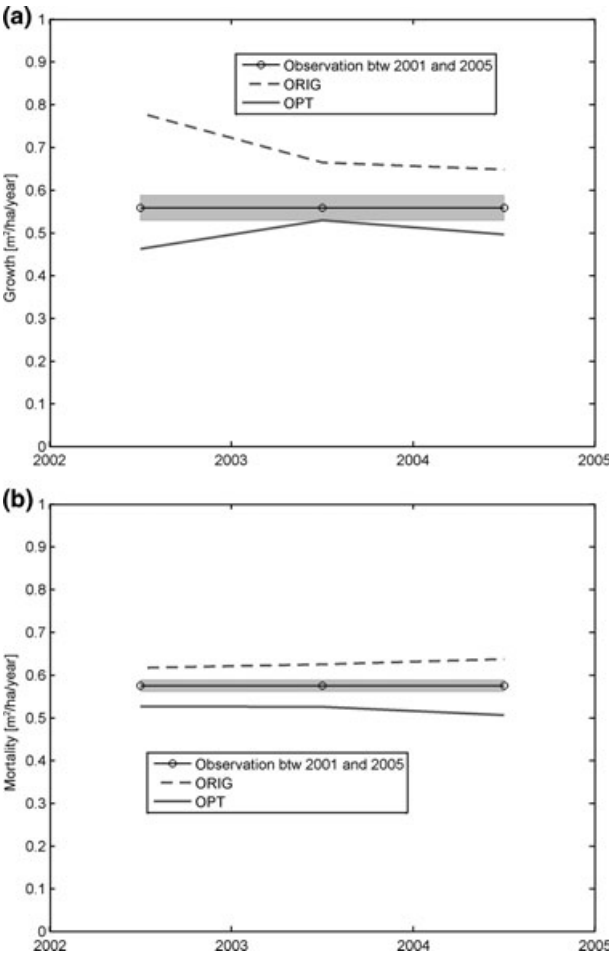

Fig. 8 Observed and predicted annual (a) growth (m^2 ha^{-1} yr^{-1}), and (b) mortality (m^2 ha^{-1} yr^{-1}). The black line shows the observations, and the shaded area indicates the 2σ error on the growth and mortality rates over the measurement interval. The dashed gray and solid gray lines, respectively, show the predictions of the ORIG and OPT model formulations. The observed rates of growth and mortality are constant throughout the simulation period because only two biometry measurements performed during this period, one in 2001 and the other in 2005, yielding a single temporally averaged growth and mortality (Rice *et al.*, 2004).

The mechanism proposed here to explain the seasonality in carbon and water fluxes observed in the Tapajos forest site is a different mechanism than that advanced by Lee *et al.* (2005) and Baker *et al.* (2008) that involves hydraulic redistribution of water within the soil column. Hydraulic redistribution has been observed in a variety species of plants (Caldwell *et al.*, 1998; Jackson *et al.*, 2000), including three species of tropical trees, but its ecosystem-scale significance in moist tropical forest ecosystems is unknown (Oliveira *et al.*, 2005). In contrast, the light-controlled phenology mechanism proposed here is supported by the empirical observations that: (1) it captures observed patterns of ecosystem-scale seasonality in NEP measured at the TNF flux tower site (Fig. 5b); and (2) the associated seasonality in leaf litter fluxes (Fig. 5a), suggesting the light-controlled phenology is an important control on the carbon fluxes of tropical forest ecosystems. As seen in Figs 5 and 6, the improvements arising from the incorporation of the light phenology scheme in capturing observed seasonality in carbon fluxes and litter fluxes. Without the light-controlled phenology, the combination of a deep soil column and dynamic water uptake is sufficient to capture the seasonality in ET (Fig. 7), but not the seasonality of litter and carbon fluxes (Figs 5 and 6).

Although this study utilized observations from a single site in the Amazon for which multiple data constraints (meteorological observations; flux tower observations; litter fluxes; and tree composition, structure, and demography measurements) were available, further evidence in support of this mechanism comes from basin-wide satellite observations over the Amazon (Myneni *et al.*, 2007), which indicate that the timing of vegetation greenness is linked to the seasonality of solar radiation across the Amazon rainforest. This implies that similar light-controlled patterns of phenology and resulting carbon and water fluxes are likely to occur across much of the Amazon region. Moreover, as we discuss in more detail in the 'Implications for long-term ecosystem dynamics' section below, the light-controlled phenology parameterization developed here also has significant implications for the climate sensitivity of the Amazon region.

Plant root water uptake

In an earlier study, Lee *et al.* (2005) showed that the strong seasonality of ET and photosynthesis in tropical regions predicted by the CLM land surface model could be reduced by allowing root hydraulic conductivity to increase with increasing depth, and allowing hydraulic redistribution between water layers. These modifications were necessary because in CLM, water uptake from each soil layer is influenced by the root fraction in the layer that declines exponentially with depth. In contrast, in ED2 water uptake from each soil layer in which a plant has roots is assumed to be dynamic, and thus determined solely by water availability, thereby allowing trees to extract available water wherever it resides (Medvigy *et al.*, 2009). Figure 7 shows the role of a deep soil column configuration by comparing the ET with two different soil depths of 1 and 6 m (used for this study), and Fig. 9 shows the available soil water in the rooting zone (i.e., 6 m). As seen in the figures, the combination of a deeper soil

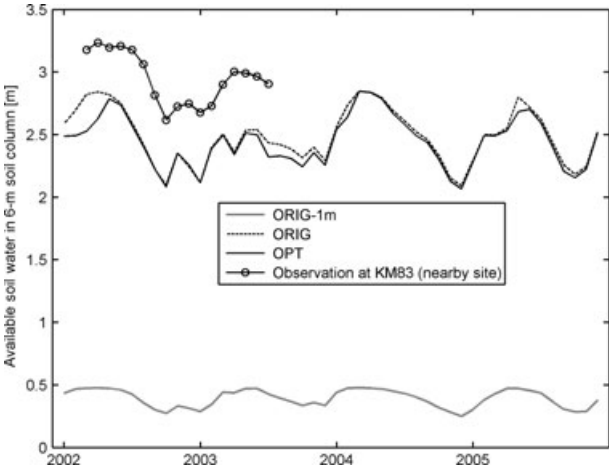

Fig. 9 Observed and predicted patterns of monthly available soil water depth. Soil water depth is estimated in 6 m soil column for ORIG, OPT, and observation, and in 1 m soil column for ORIG-1m. The black line with circles shows the observations at the nearby site (KM83; 3.01°S, 54.58°W) in Tapajos National Forest (TNF) (data from Bruno *et al.*, 2006). The solid gray, dashed black, and solid black lines, respectively, show the predictions of the ORIG-1m, ORIG, and OPT model formulations.

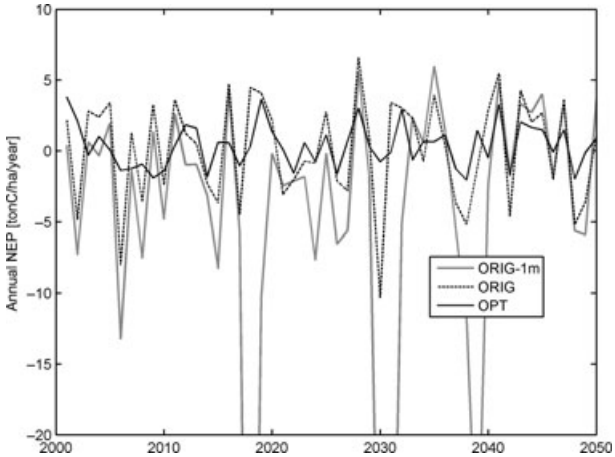

Fig. 10 Interannual variability of net ecosystem productivity (NEP, tonC ha^{-1} yr^{-1}) from 2000 to 2050. The simulations are forced with CCSM SRES A2 climate change scenario. The solid gray, dashed black, and solid black lines, respectively, show the predictions of the ORIG-1m, ORIG, and OPT model formulations.

column and dynamic water uptake enables ED2 to capture the observed seasonality of ET even in the absence of hydraulic redistribution. These findings are consistent with the findings of Zheng & Wang (2007), who incorporated a similar dynamic water uptake formulation into CLM3 and IBIS2 and showed that when combined with a sufficiently deep soil column, both models had significantly improved predictions of ET fluxes in the absence of hydraulic redistribution. As the results of the analysis presented here show, however, even with the correct pattern of seasonality in ET, the correct pattern of seasonality in ecosystem carbon fluxes and litter fluxes is only captured after incorporating a light-dependent model of leaf phenology (Figs 5 and 6).

Implications for long-term ecosystem dynamics

A significant number of atmospheric general circulation (GCM) models predict a drying of the Amazon region in response to increasing anthropogenic CO_2 emissions (Malhi *et al.*, 2009). In particular, the Hadley Centre GCM (HadCM3) predicts a major loss of Amazon under climate change scenarios (Cox *et al.*, 2000; Huntingford *et al.*, 2008). To evaluate the impact of the light-controlled leaf phenology scheme on the resilience of Amazon forest ecosystem function, we performed a series of simulations with CCSM SRES A2 climate change scenario from 2001 to 2050. As shown in Fig. 10, incorporating light-controlled phenology into the model reduces the interannual variability in carbon fluxes, indicating that, at least at this timescale, light-controlled phenology acts a source of resilience to the impacts of climate variability on tropical carbon fluxes. The dry-season leaf flushing both moderates the seasonality of carbon fluxes and reduces the interannual variability of carbon fluxes. This result implies that leaf responses to the dry season are likely to have important implications for the sensitivity of Amazon forests to interannual variability in climate forcing. To the extent that the environmental sensitivity of the plants represented in model formulation reflects that observed in the field, it implies that the seasonal green-up of the plant canopy is relevant to the recent controversy about the drought sensitivity of the Amazon. Saleska *et al.* (2007) argued that MODIS EVI indicated a green-up of Amazon forests during the 2005 drought; however, Samanta *et al.* (2010) claimed the results of Saleska *et al.* (2007) were not reproducible due to atmosphere-corrupted data. Using remotely sensed EVI measurements to infer basin-wide phonological patterns is complicated, however, since its seasonal variability does not follow the seasonality of radiation, precipitation or litter fluxes. Two important lines of further investigation will be to assess whether the model's predictions of interannual variability in carbon fluxes are consistent with observed levels of interannual variability, and to assess the regional-scale applicability of the model formulation using data from other sites across the region.

Acknowledgements

The authors would like to acknowledge the National Science Foundation (NSF) ATM-0450307 and ATM-0449793, entitled

'Collaborative Research: WCR: Is Deforestation Changing the Hydrologic Climate and Vegetation Dynamics of the Amazon'. We thank David Fitzjarrald at University of Albany, SUNY, for providing the radiation data. We also thank Humberto Ribeiro da Rocha at University of Sao Paulo for providing the soil moisture data, collected at the KM83 site in TNF.

References

Albani M, Medvigy D, Hurtt GC, Moorcroft PR (2006) The contributions of land-use change, CO_2 fertilization, and climate variability to the Eastern US carbon sink. *Global Change Biology*, **12**, 2370–2390.

Aranibar JN, Berry JA, Riley WJ, Pataki DE, Law BE, Ehleringer JR (2006) Combining meteorology, eddy fluxes, isotope measurements, and modeling to understand environmental controls of carbon isotope discrimination at the canopy scale. *Global Change Biology*, **12**, 710–730.

Baker IT, Prihodko L, Denning AS, Goulden M, Miller S, Da Rocha HR (2008) Seasonal drought stress in the Amazon: reconciling models and observations. *Journal of Geophysical Research-Biogeosciences*, **33**, G00B01.

Bruno RD, Da Rocha HR, De Freitas HC, Goulden ML, Miller SD (2006) Soil moisture dynamics in an eastern Amazonian tropical forest. *Hydrological Processes*, **20**, 2477–2489.

Caldwell MM, Dawson TE, Richards JH (1998) Hydraulic lift: consequences of water efflux from the roots of plants. *Oecologia*, **113**, 151–161.

Chave J, Muller-Landau HC, Baker TR, Easdale TA, Ter Steege H, Webb CO (2006) Regional and phylogenetic variation of wood density across 2456 neotropical tree species. *Ecological Applications*, **16**, 2356–2367.

Cox PM, Betts RA, Jones CD, Spall SA, Totterdell IJ (2000) Acceleration of global warming due to carbon-cycle feedbacks in a coupled climate model. *Nature*, **408**, 184–187.

Domingues TF, Berry JA, Martinelli LA, Ometto J, Ehleringer JR (2005) Parameterization of canopy structure and leaf-level gas exchange for an eastern Amazonian tropical rain forest (Tapajos National Forest, Para, Brazil). *Earth Interactions*, **9**, 1–23.

Edwards AWF (1972) *Likelihood*. Cambridge, Cambridge University Press.

Foley JA, Prentice IC, Ramankutty N, Levis S, Pollard D, Sitch S, Haxeltine A (1996) An integrated biosphere model of land surface processes, terrestrial carbon balance, and vegetation dynamics. *Global Biogeochemical Cycles*, **10**, 603–628.

Freeland RO (1952) Effect of age of leaves upon the rate of photosynthesis in some conifers. *Plant Physiology*, **27**, 685–690.

Gaudinski JB, Trumbore SE, Davidson EA, Zheng S (2000) Soil carbon cycling in a temperate forest: Radiocarbon-based estimates of residence times, sequestration rates and partitioning of fluxes. *Biogeochemistry*, **51**, 33–69.

Gill RA, Jackson RB (2000) Global patterns of root turnover for terrestrial ecosystems. *New Phytologist*, **147**, 13–31.

Huete AR, Didan K, Shimabukuro YE *et al.* (2006) Amazon rainforests green-up with sunlight in dry season. *Geophysical Research Letters*, **33**, L06045.

Huete AR, Restrepo-Coupe N, Ratana P *et al.* (2008) Multiple site tower flux and remote sensing comparisons of tropical forest dynamics in Monsoon Asia. *Agricultural and Forest Meteorology*, **148**, 748–760.

Huntingford C, Fisher RA, Mercado L *et al.* (2008) Towards quantifying uncertainty in predictions of Amazon 'dieback'. *Philosophical Transactions of the Royal Society B-Biological Sciences*, **363**, 1857–1864.

Hurtt GC, Pacala SW, Moorcroft PR, Caspersen J, Shevliakova E, Houghton RA, Moore B (2002) Projecting the future of the US carbon sink. *Proceedings of the National Academy of Sciences of the United States of America*, **99**, 1389–1394.

Hutyra LR, Munger JW, Saleska SR *et al.* (2007) Seasonal controls on the exchange of carbon and water in an Amazonian rain forest. *Journal of Geophysical Research-Biogeosciences*, **112**, G03008.

Jackson RB, Sperry JS, Dawson TE (2000) Root water uptake and transport: using physiological processes in global predictions. *Trends in Plant Science*, **5**, 482–488.

Lee JE, Oliveira RS, Dawson TE, Fung I (2005) Root functioning modifies seasonal climate. *Proceedings of the National Academy of Sciences of the United States of America*, **102**, 17576–17581.

Luizao FJ (1989) Litter production and mineral element input to the forest floor in a Central Amazonian forest. *GeoJournal*, **19**, 407–417.

Mahadevan P, Wofsy SC, Matross DM *et al.* (2008) A satellite-based biosphere parameterization for net ecosystem CO2 exchange: Vegetation Photosynthesis and Respiration Model (VPRM). *Global Biogeochemical Cycles*, **22**, GB2005.

Malhi Y, Aragão LEOC, Galbraith D *et al.* (2009) Exploring the likelihood and mechanism of a climate-change-induced dieback of the Amazon rainforest. *Proceedings of the National Academy of Sciences*, **106**, 20610–20615.

Matamala R, Gonzàlez-Meler MA, Jastrow JD, Norby RJ, Schlesinger WH (2003) Impacts of fine root turnover on forest NPP and soil C sequestration potential. *Science*, **302**, 1385–1387.

Medvigy D, Wofsy SC, Munger JW, Hollinger DY, Moorcroft PR (2009) Mechanistic scaling of ecosystem function and dynamics in space and time: Ecosystem Demography model version 2. *Journal of Geophysical Research-Biogeosciences*, **114**, G01002.

Miranda LDPD, Vitória AP, Funch LS (2011) Leaf phenology and water potential of five arboreal species in gallery and montane forests in the Chapada Diamantina; Bahia; Brazil. *Environmental and Experimental Botany*, **70**, 143–150.

Moorcroft PR (2003) Recent advances in ecosystem-atmosphere interactions: an ecological perspective. *Proceedings of the Royal Society B-Biological Sciences*, **270**, 1215–1227.

Moorcroft PR (2006) How close are we to a predictive science of the biosphere? *Trends in Ecology & Evolution*, **21**, 400–407.

Moorcroft PR, Hurtt GC, Pacala SW (2001) A method for scaling vegetation dynamics: the ecosystem demography model (ED). *Ecological Monographs*, **71**, 557–585.

Myneni RB, Yang WZ, Nemani RR *et al.* (2007) Large seasonal swings in leaf area of Amazon rainforests. *Proceedings of the National Academy of Sciences of the United States of America*, **104**, 4820–4823.

Nepstad DC, Decarvalho CR, Davidson EA *et al.* (1994) The role of deep roots in the hydrological and carbon cycles of Amazonian forests and pastures. *Nature*, **372**, 666–669.

Oliveira RS, Dawson TE, Burgess SSO, Nepstad DC (2005) Hydraulic redistribution in three Amazonian trees. *Oecologia*, **145**, 354–363.

Pyle EH, Santoni GW, Nascimento HEM *et al.* (2008) Dynamics of carbon, biomass, and structure in two Amazonian forests. *Journal of Geophysical Research-Biogeosciences*, **113**, G00B08.

Rice AH, Pyle EH, Saleska SR *et al.* (2004) Carbon balance and vegetation dynamics in an old-growth Amazonian forest. *Ecological Applications*, **14**, S55–S71.

Rivera G, Elliott S, Caldas LS, Nicolossi G, Coradin VT, Borchert R (2002) Increasing day-length induces spring flushing of tropical dry forest trees in the absence of rain. *Trees – Structure and Function*, **16**, 445–456.

Saldarriaga JG, West DC, Tharp ML, Uhl C (1988) Long-term chronosequence of forest succession in the upper Rio Negro of Columbia and Venezuela. *Journal of Ecology*, **76**, 938–958.

Saleska SR, Miller SD, Matross DM *et al.* (2003) Carbon in amazon forests: unexpected seasonal fluxes and disturbance-induced losses. *Science*, **302**, 1554–1557.

Saleska SR, Didan K, Huete AR, Da Rocha HR (2007) Amazon forests green-up during 2005 drought. *Science*, **318**, 612–612.

Samanta A, Ganguly S, Hashimoto H *et al.* (2010) Amazon forests did not green-up during the 2005 drought. *Geophysical Research Letters*, **37**, L05401.

Silver WL, Neff J, Mcgroddy M, Veldkamp E, Keller M, Cosme R (2000) Effects of soil texture on belowground carbon and nutrient storage in a lowland Amazonian forest ecosystem. *Ecosystems*, **3**, 193–209.

Stöckli R, Lawrence DM, Niu GY *et al.* (2008) Use of FLUXNET in the community land model development. *Journal of Geophysical Research-Biogeosciences*, **113**, G01025.

Trumbore S, Da Costa ES, Nepstad DC *et al.* (2006) Dynamics of fine root carbon in Amazonian tropical ecosystems and the contribution of roots to soil respiration. *Global Change Biology*, **12**, 217–229.

Van Schaik CP, Terborgh JW, Wright SJ (1993) The phenology of tropical forests: adaptive significance and consequences for primary consumers. *Annual Review of Ecology and Systematics*, **24**, 353–377.

Werth D, Avissar R (2004) The regional evapotranspiration of the Amazon. *Journal of Hydrometeorology*, **5**, 100–109.

Wright SJ, Cornejo FH (1990) Seasonal drought and leaf fall in a tropical forest. *Ecology*, **71**, 1165–1175.

Wright SJ, Van Schaik CP (1994) Light and the phenology of tropical trees. *American Naturalist*, **143**, 192–199.

Wright IJ, Reich PB, Westoby M *et al.* (2004) The worldwide leaf economics spectrum. *Nature*, **428**, 821–827.

Xiao XM, Zhang QY, Saleska S *et al.* (2005) Satellite-based modeling of gross primary production in a seasonally moist tropical evergreen forest. *Remote Sensing of Environment*, **94**, 105–122.

Zheng Z, Wang G (2007) Modeling the dynamic root water uptake and its hydrological impact at the Reserva Jaru site in Amazonia. *Journal of Geophysical Research-Biogeosciences*, **112**, G04012.

Supporting Information

Additional Supporting Information may be found in the online version of this article:

Appendix S1. Soil decomposition.
Appendix S2. Allocation.
Appendix S3. Growth.
Appendix S4. Mortality.
Appendix S5. Model fitting procedures.
Appendix S6. References.

Please note: Wiley-Blackwell are not responsible for the content or functionality of any supporting materials supplied by the authors. Any queries (other than missing material) should be directed to the corresponding author for the article.